Resistivities of conductive composites

G. R. Ruschau, S. Yoshikawa, and R. E. Newnham

Citation: Journal of Applied Physics **72**, 953 (1992);
View online: https://doi.org/10.1063/1.352350
View Table of Contents: http://aip.scitation.org/toc/jap/72/3
Published by the American Institute of Physics

Resistivities of conductive composites

G. R. Ruschau,[a] S. Yoshikawa, and R. E. Newnham
Materials Research Laboratory, Pennsylvania State University, University Park, Pennsylvania 16802

(Received 10 February 1992; accepted for publication 22 April 1992)

A steady-state model for the resistivity of composites is presented, based on the idea that the resistance through a composite is the result of a series of a large number of resistors combined in series and parallel. There are three separate contributions to the resistance: constriction resistance at the contacts, tunneling resistance at the contacts, and the intrinsic filler resistance through each particle, with tunneling resistance generally dominating the magnitude of the overall resistance. The model predicts resistivity increases with increasing filler hardness and/or elastic modulus and insulating film thickness, while resistivity decreases with increasing particle size and intrinsic stress. The room-temperature dc resistivity behavior of conductor-filled silicone rubber composites was investigated to verify the model. Comparison of the model to this experimental data showed that good agreement could be obtained for filler materials in which the tarnish layer was a known quantity for a given powder; for other cases, the experimental values were higher than predicted.

I. INTRODUCTION

Composites consisting of highly conductive filler powder dispersed in a flexible, insulating polymer matrix are commonly used in electronic applications for die attach,[1] solderless connectors,[2] thermistors,[3,4] and pressure-sensing elements.[5] Other uses of such composites include electromagnetic shielding and antistatic devices[6] as well as chemical sensors.[7]

The properties of composite systems are understood in terms of percolation phenomena; when a sufficient amount of conductive filler is loaded into an insulating polymer matrix, the composite transforms from and insulator to a conductor, the result of continuous linkages of filler particles. This is shown graphically in Fig. 1; as the volume fraction of filler is increased, the probability of continuity increases until the critical volume fraction, beyond which the electrical conductivity is high, comparable to the filler material. Effective-media theories attempt to quantify the resistance of these systems, based on the idea that the contribution of each phase to the conductivity depends not only on the relative amount of that phase present but also its degree of self-connectivity. A number of effective-media equations have been derived to model the shape of this curve;[8–11] while these equations can successfully mimic this shape, they are not useful for describing the magnitude of the electrical resistivity of the composite.

Once percolation is "complete," i.e., a significant number of percolated linkages has formed, the differences in conductivity between samples with the same degree of self-connectivity and the same volume fraction of filler but with different filler materials can be unpredictably large. All particle-filled composites have resistivities several orders of magnitude higher than the resistivities of the pure filler materials. This has been well documented for a variety of conductive fillers, as shown in Table I. In many cases, it is difficult to obtain composites with resistivities within five orders of magnitude of the pure material.

In a previous paper,[14] the authors presented a model showing the dependence of composite resistivity on filler particle size to help quantify the differences. In this investigation, this model has been expanded to include the fundamentals of contact resistance; a more accurate model was derived from these principles.

II. DERIVATION OF THE MODEL

A. Fundamentals of contact resistance

When speaking of effective-media approximations in electrically conductive composites, a continuous linkage of conductive particles is often thought of as a single conductive filament; however, this is not accurate. Rather, each percolated linkage should be thought of as a series of resistors, with each particle and each particle-particle contact contributing to the total resistance in the filament. There are two important contributions to the particle-particle contact resistance: constriction resistance and tunneling resistance.

1. Constriction resistance

When two conductive spheres meet, there is a resistance associated with the constriction of electron flow through the small area. This resistance, known as the constriction resistance R_{cr}, can be derived from the principles of ohmic conduction and electric fields, and has been shown[15] to be

$$R_{cr}=\rho_i/d, \tag{1}$$

where ρ_i is the intrinsic filler resistivity and d is the diameter of the contact spot. Intuitively, this is a surprising result in that R_{cr} is inversely proportional to the diameter, rather than the area, of the contact spot. For a composite with a filler of a given particle size D, the important relationship is the ratio of D/d; when this ratio $> \sim 10$, Eq.

[a]Permanent address: ARCO Oil & Gas, 2300 W. Plano Pkwy, Plano, TX 75075.

 0021-8979/92/150953-07$04.00

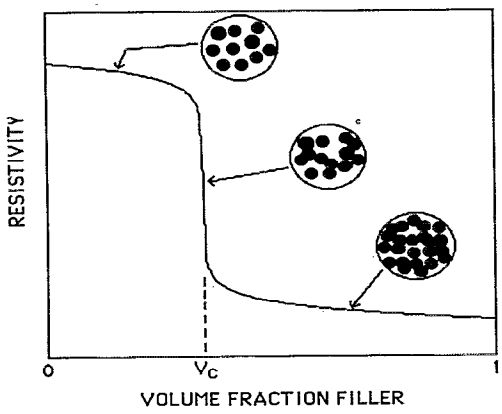

FIG. 1. Percolation theory, as applied to conductive composites. The formation of the first complete particle linkage results in a sharp drop in resistivity at V_c.

(1) begins to diverge so that very high resistances result even though the spheres may still be in physical contact.

2. Tunneling resistance

The other important limitation to the conductivity of two spheres is the resistance associated with any insulating film which may be completely coating each filler particle. The origin of this film may vary somewhat depending on the system. Tarnish films on metals are known to form almost instantly upon exposure of a pristine metal surface to normal atmospheric conditions.

Such oxide films, over a reasonably short period of time, may be somewhat protective so that a limiting, transient film thickness may be assumed for a given metal. For metals that obey the logarithmic law, the oxide is very protective and the transient film thicknesses (and their contribution to the tunneling resistivity) are easier to predict. In reality, the initial oxide formation is a very complicated issue, depending on the partial pressure of oxygen, the crystallographic orientation of the metal surface, the stoichiometry of the oxide formed (i.e., Cu_2O vs CuO), the relative humidity, etc.[16]

TABLE I. Resistivities of conductor-filled polymers by other investigators.

Filler	Polymer	Filler resistivity (mΩ cm)[a]	Composite resistivity (mΩ cm)[b]	Vol % loading
C black	Polyethylene	1.0	2000	30[c]
V_2O_3	Polyethylene	0.1–10.0	100 000	50[d]
$MoSi_2$	Polyethylene	0.021	500 000	50[e]
TiB_2	Polyethylene	0.028	60 000	40[e]
Fe	Styrene/Acrylonitrile	0.010	1 000 000	50[f]
Al	Polypropylene	0.003	20 000	25[f]
Cu	Polyvinyl chloride	0.002	600	20[g]
Ag	Epoxy resin	0.002	1.0	50[h]

[a]Theoretical.
[b]Experimental.
[c]See Ref. 4.
[d]See Ref. 3.
[e]See Ref. 12
[f]See Ref. 6.
[g]See Ref. 13.
[h]See Ref. 1

For processed powders, residual organic films may remain on the powder surface after milling, sometimes purposely deposited for dispersion or dedusting reasons. Further processing in organic solutions may or may not remove these films. In a conductor-filled polymer composite, the polymer itself may completely cover the powder surface, resulting in a thin film of polymer separating the powders.

All three of these films may be present in varying thicknesses, providing an insulating layer between two spheres. According to classical mechanics (and the Bruggeman asymmetric effective media[9] or Hashin coated-spheres models[10]), this would result in a high series resistance, but this is not the case. For thin films on the order of 100 Å or less, quantum-mechanical tunneling can occur, resulting in lower resistivities.

The physics of quantum-mechanical tunneling show that the relative probability that an electron will "tunnel through," rather than surmount, a potential barrier is proportional to the work function of the conductor, the thickness of the film, and the relative dielectric permittivity of the film. The surprising result is that the resistivity of the film is not a factor in tunneling, so that organics, polymers, and oxides, most with similar work functions and permittivities, will have similar tunneling resistivities for similar film thicknesses.

The dependence of tunneling resistivity on the insulating film thickness has been derived mathematically. Dietrich[17] pioneered the work on this problem, and presented a general tunneling curve (based on TiO_2 films on Ti), empirically derived but thought to be approximately applicable to all materials (see Fig. 2).

Thus a tunneling resistivity ρ_t may be applied to the contact if the insulating film thickness is known. The tunneling resistance associated with a contact R_t is, unlike constriction resistance, inversely proportional to the contact spot area a, so

$$R_t = \rho_t / a. \tag{2}$$

The resistance of a contact therefore is the sum of these two separate effects,

$$R_c = \rho_i / d + \rho_t / a. \tag{3}$$

In general, the tunneling resistance term dominates R_c except in the cases of noble metals or carefully cleaned and protected metal contact surfaces.

3. Contact spots

There is still an unknown quantity in Eq. (3), that being the contact spot area [or diameter, but obviously $d = (4a/\pi)^{1/2}$ for spherical particles with circular contact spots]. This area must be a function of the applied pressure between particles F and the deformation that occurs as a result of this applied pressure.

There are two types of deformation that can occur when two particles come into contact, elastic (recoverable) and plastic (permanent) deformation. Wagar[18] showed that in the case of electrical contacts, the strains necessary to reduce the constriction resistance below the critical

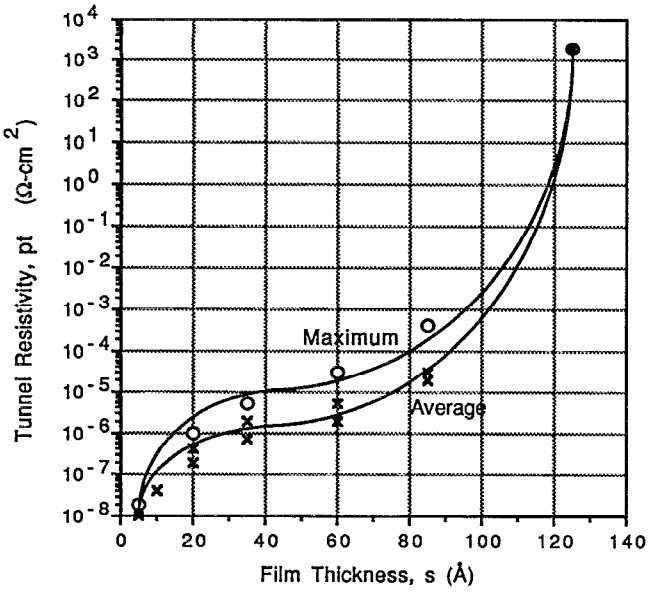

FIG. 2. Tunnel resistivity for thin films of TiO_2 on Ti as a function of film thickness (Ref. 17).

value of ~10 are larger than the elastic yield strain; that is, if "good" electrical contact is made, both elastic and plastic deformation occur.

The magnitude of the deformation for a given force is controlled by a material parameter, the contact hardness H, which is either measured by observing areas of indentation under applied load or approximated by taking $H=3\sigma y$, where σy=the 0.2% offset yield stress. Though "hardness" is generally defined as a measure of the tendency of a material to bulk or volume flow, contact hardness is not always easy to define. When thick oxide films grow on metals, for example, the measured hardness will vary depending on the method used for measurement; microhardness techniques would obviously be more sensitive to thin oxide film properties than ordinary stress/strain curve approximations. In addition, work hardening of metals results in harder, stiffer materials due to an increase in dislocation densities, so the history of a specific metal powder is important.

Despite these inconsistencies, the area of contact between two spheres can be fairly accurately determined by one of the following:

$$a=F/H \quad \text{(plastic case)}, \tag{4a}$$

$$a=2.43(FD/E)^{2/3} \quad \text{(elastic case)}, \tag{4b}$$

where D is the sphere diameter and E is the elastic modulus. Since in most cases the deformation is a combination of plastic and elastic regions, the empirical term ξ, called the elasticity factor, is introduced. For the combination of elastic and plastic deformation the contact area becomes

$$a=F/\xi H. \tag{5}$$

ξ ranges from a value of 0.2 for purely elastic deformation to 1.0 for purely plastic deformation. For most systems, a value of $\xi=0.7$ has been found to be quite reliable.

Substituting Eq. (5) into Eq. (3) gives

$$R_{c\ (\text{plastic})}=0.89\rho_i(\xi H/F)^{1/2}+\rho_t\xi H/F, \tag{6a}$$

while substituting Eq. (4b) into Eq. (3) for elastic deformation gives

$$R_{c\ (\text{elastic})}=0.57\rho_i(E/FD)^{1/3}+0.26\rho_t(E/FD)^{2/3}. \tag{6b}$$

This describes the resistance at an electrical contact in terms of some known material parameters and the (variable) applied force.

III. APPLYING CONTACT RESISTANCE TO COMPOSITES

In composite conductors the total resistance is a function of both the resistance through each particle and the particle-particle contact resistance. The number of contacts between electrodes thus becomes a factor in this relationship, as well as the number of conduction paths. If contact resistance at the electrodes is also considered, the resistance may be described by the following relation, developed by Yasuda and Nagata:[19]

$$R_c=2R_e+\frac{(M-1)R_p+MR_i}{N}, \tag{7}$$

where R_c is the composite resistance, R_e the lead resistance to electrodes, R_p the particle-particle contact resistance, R_i the resistance across one particle, M the number of particles forming one conduction path, and N the number of conduction paths. If a four-point-probe resistance measurement is used, R_e is eliminated from Eq. (7).

For highly conductive composites, the volume loading is high enough to avoid percolation threshold effects, and in this case the maximum number of particles is involved in the electrical conductivity. Thus, this type of composite may properly be thought of as a true conductive skeleton of a certain packing geometry.

Consider the simplest form of skeleton geometry, simple cubic packing. For a composite of length L, width w, and thickness t with electrodes at both ends (see Fig. 3) and monosized spheres arranged in simple cubic packing, the number of conductive chains between the electrodes is simply the cross-section area of the sample divided by the cross-section area of one chain. If the particle diameter is given by d, then the cross-section area of one chain and its surrounding insulation is d^2, and thus

$$N=wt/d^2. \tag{8}$$

Similarly, the number of particles in one chain is given by the distance between electrodes divided by the particle diameter, or

$$M=L/d. \tag{9}$$

These simplifying assumptions do not adequately describe the arrangement of conductive chains in a real composite. In an actual sample, the conductive pathways may meander from the straight, parallel arrangement assumed above. For comparison purposes, however, the assumptions are necessary.

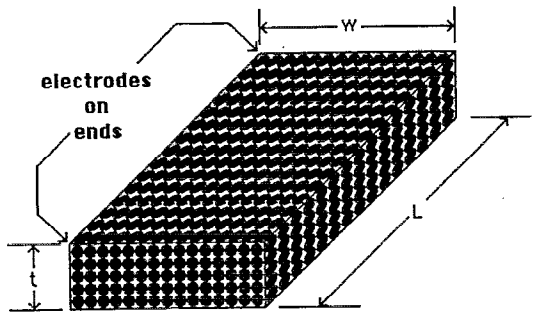

FIG. 3. Composite sample with smple cubic packing.

For samples in which the L/d ratio is large, it is convenient to make the simplifying assumption

$$M-1\approx M. \tag{10}$$

The intrinsic resistance of an individual particle may be estimated assuming an equivalent cross-sectional area of a sphere, that is, the cross-sectional area of a cylinder whose volume is equal to the sphere. By geometry, this cross-sectional area can be shown to be $0.524d^2$. Given that the resistance across the particle is related to the intrinsic resistvity ρ_i, by $R_i = \rho_i/(wt/L)$, with $wt = 0.524d^2$ and $L=d$, this leads to the relation

$$R_i=\rho_i(d/0.524d^2)=\rho_i/0.524d. \tag{11}$$

The validity of the equivalent cross-sectional area assumption may be questionable but, as will be shown, it is of little significance in the model.

Substituting Eqs. (8), (9), (10), and (11) into Eq. (7) gives

$$R_c=(Ld/wt)R_p+(L/wt)\rho_i/0.524. \tag{12}$$

From Eq. (6a), R_p may be assumed to be equivalent to the general case for contact resistance of plastically deformed spheres,

$$R_{p\ (\text{plastic})}=0.89\rho_i(\xi H/F)^{1/2}+\rho_t\xi H/F, \tag{13a}$$

where ξ is the elasticity factor $(0.2<\xi<1.0)$, H is the contact hardness, and F is the applied contact force.

The strains associated with electrical contact in a composite may be purely elastic in nature; certainly this is the case for ceramic fillers that undergo little or no plastic deformation. In this case Eq. (6b) applies,

$$R_{p\ (\text{elastic})}=0.57\rho_i\left(\frac{E}{FD}\right)^{1/3}+0.26\rho_t\left(\frac{E}{Fd}\right)^{2/3}. \tag{13b}$$

Equations (13a) and (13b) describe the resistance of each particle-particle contact for the elastic/plastic and pure elastic cases, respectively. Applied to a composite that contains N contacts in its cross-sectional area, M contacts in series, and a contact force of F/N, R_p can be expressed as R_p' [$= (Ld/wt)R_p$], the total resistance due to all particle-particle contacts. Equations (13a) and (13b) then become

$$R_{p\ (\text{plastic})}'=0.89\rho_i L(\xi H/Fwt)^{1/2}+\rho_t\xi HL/Fd, \tag{14a}$$

$$R_{p\ (\text{elastic})}'=0.57\rho_i L(E/F)^{1/3}[1/(wt)^{2/3}]+0.26\rho_t L[1/d(wt)^{1/3}](E/F)^{2/3}. \tag{14b}$$

Substituting into Eq. (12) yields

$$R_{c\ (\text{plastic})}=0.89\rho_i L(\xi H/Fwt)^{1/2}+\rho_t\xi HL/Fd+(L/wt)\rho_i/0.524, \tag{15a}$$

$$R_{c\ (\text{elastic})}=0.57\rho_i L(E/F)^{1/3}[1/(wt)^{2/3}]+0.26\rho_t L[1/d(wt)^{1/3}](E/F)^{2/3}+(L/wt)\rho_i/0.524. \tag{15b}$$

This describes the resistance of a composite in terms of sample geometry, particle size, applied force, and the intrinsic properties of the conductive filler.

To express this in terms of the specific electrical resistivity of the composite ρ_c, multiplying both sides of Eqs. (15a) and (15b) by (wt/L) yields

$$\rho_{c\ (\text{plastic})}=0.89\rho_i(\xi Hwt/F)^{1/2}+\rho_t\xi Hwt/Fd+\rho_i/0.524 \tag{16a}$$

$$\rho_{c\ (\text{elastic})}=0.57\rho_i(Ewt/F)^{1/3}+(0.26\rho_t/d)(Ewt/F)^{2/3}+\rho_i/0.524. \tag{16b}$$

Equation (16a) may be more appropriate for metal and polymer fillers, while Eq. (16b) applies to ceramics.

The following assumptions are inherent in this model.

(i) The volume fraction occupied by the filler is 0.524 and is independent of particle size; this is not true for real systems, but it is true under the stated ideal conditions (perfect spheres with simple cubic packing). This is not the critical volume fraction for conduction as described by percolation theory, but is instead the volume fraction for the complete conductive skeleton. Rough estimates of percolation effects on resistivity based on the volume fraction for a particular sample V_f can be made by multiplying the calculated resistivities by $0.524/\phi_p$. This accounts for the decreased number of percolated pathways in the less heavily loaded yet highly conductive composites. The model is only meant to offer a qualitative look at the factors affecting resistance and a quantitative comparison of two different filler materials with regard to their intrinsic properties.

(ii) All particles are involved in conduction, i.e., no "cul de sacs" (nonpercolated chains) exist. Therefore, the model is only valid for samples that are thick enough to avoid the effects of cul de sacs (large ratio of t/d). The conduction paths are straight chains, not meandering randomly through the composite.

(iii) The tunneling resistivity and contact force are the same for any two particles of the same material, independent of particle size; only the contact areas are different (i.e., all contacts within a composite are the same).

(iv) The electrical resistivity of the polymer and tunneling conduction through regions other than at the particle-particle interface do not significantly figure into the resistivity of the composite when there is percolation.

A. Intrinsic stress in composites

The sample dimensions wt appear in both Eqs. (16a) and (16b), indicating that resistivity is a function of sample geometry. This, however, is purely a mathematical consequence of the model; resistivity is a function of wt only in cases where a known constant contact force F is applied (e.g., a fixed weight placed on top of a loose powder). For composites, the geometry dependence of the resistivity can be eliminated by substituting an induced stress σ_i into the model for resistivity.

There are several contributions to σ_i. First of all, when a filler that has a lower coefficient of thermal expansion than the polymer matrix is introduced into the matrix, tensile stress will be induced in the polymer when the composite is cooled. The thermally generated stress σ^* can be calculated directly for polymers that are below T_g or T_m and spherical fillers.[20] In the case of thermally cured composites or composites that are mixed in the molten state of the polymer, σ^* is a function of the difference in thermal-expansion coefficients and the reference temperature in the form.

$$\sigma^* = KE(\alpha_p - \alpha_f)(T_0 - T), \tag{17}$$

where K is a constant (≈ 1), E is the composite modulus in an unstressed state, [many different approximations available—series model: $E = V_f E_f + (1 - V_f)E_p$], α_p is the thermal-expansion coefficient of the polymer, α_f is the thermal-expansion coefficient of the filler, T_0 is the temperature at which thermal stresses set in (usually T_g or T_m), and T is the reference temperature.

For example, 25% silver filler ($\alpha_f = 57 \times 10^{-6}$/°C, $E_f = 76 \times 10^9$ N/m^2) in polystyrene ($T_0 = T_g \sim 105$ °C, $\alpha_p = 1.9 \times 10^{-4}$/°C, $E_p = 3.4 \times 10^9$ N/m^2) produces a thermal stress of 2.3×10^8 N/m^2 at 25 °C.

When $T > T_g$, which is the case with elastomers, the thermally induced stress is relaxed out of the composite with time. Nonetheless, stresses that were quickly relieved may be large enough to cause the initial deformation in the filler material. In addition, when sufficiently crosslinked, complete stress relaxation cannot occur even well above T_g; this is why rubber bands maintain their elasticity over long periods of time.[21] For elastomers, therefore, σ^* depends on the cooling rate and the dynamic mechanical properties of the polymer; if the time to cooling is faster than the relaxation time of the polymer, an initial stress will occur.

Another source of internal stress is capillary action. When two particles have an intervening bridge of liquid between them, the particles will be pulled together with sufficient force so as to minimize the liquid-vapor surface area. The magnitude of the force depends on the curvature of the liquid surface, the surface energy, and the liquid volume. The greater the curvature and surface energies, and the smaller the liquid volume, the greater the capillary force.[22]

In addition to thermally generated stresses and stresses induced by capillary action, the stress induced by shrinkage crosslinking provides another contribution to σ_i. This effect has been shown to be significant in filled epoxies.[23] Because crosslinking decreases the free volume of a polymer, an increase in T_g can be seen for crosslinked systems, with the increase proportional to the crosslink density. Therefore, crosslinking also increases the thermally generated stress, as calculated by Eq. (17).

Substituting σ_i for F/wt in the models leaves

$$\rho_{c\ (\text{plastic})} = 0.89\rho_i(\xi H/\sigma_i)^{1/2} + \rho_t \xi H/d\sigma_i + \rho_i/0.524, \tag{18a}$$

$$\rho_{c\ (\text{elastic})} = 0.57\rho_i(E/\sigma_i)^{1/3} + (0.26\rho_t/d)(E/\sigma_i)^{2/3} + \rho_i/0.524. \tag{18b}$$

In the case of only elastic deformation of the filler in an elastomer matrix, the force due to σ_i must be greater than the elastic restoring force of the filler, or else only point contact is possible. Electron tunneling is still possible over a distribution of gap widths, but this is not accounted for in the model, as noted in the model assumptions given previously.

The implications of this model for producing composites are clear, and the number of controlling parameters is surprisingly low (although percolation considerations, not discussed here, present a separate set of variables which depend on several other factors[8]). The model predicts resistivity increases with increasing filler hardness and/or elastic modulus and insulating film thickness, while resistivity decreases with increasing particle size and intrinsic stress. Thus to produce the most highly conductive composite, it is necessary to choose relatively soft, large particle size fillers; conductor-coated polymeric fillers provide a good combination of softness without losing the intrinsic conductivity of the metal, while long, fibrous fillers result in fewer particle-particle contacts in series to reduce the overall contribution of the contact resistance. Small transient oxide or tarnish layers are especially critical, particularly for large-scale sample preparation in which the powders cannot be cleaned before processing. Finally, it is beneficial to use polymer matrices that undergo considerable shrinkage during processing, such as semicrystalline polymers which generally undergo a large, abrupt volume change at the crystalline melting point.

B. Coated fillers

For situations in which a nonconductive filler material is coated with a conductor, each particle becomes a more complex version of two individual resistors combined in parallel. Hashin[10] developed the relationship to predict the resistivity ρ_{cs} of conductor-coated spheres. This coated-spheres model (which has also been used as an effective-media approximation for composites as a whole) is as follows:

$$\rho_{cs} = \rho_{coat}\left(1 + \frac{V_{core}}{[(\rho_{coat}/\rho_{core}) - 1]^{-1} + (1 - V_{core})/3}\right)^{-1}, \tag{19}$$

where V_{core} is the volume fraction of the sphere occupied by core, ρ_{coat} is the resistivity of the coating material, and

TABLE II. Intrinsic properties of filler materials and substrates used in model for resistivity.

Filler	Manufacturer	ρ_i ($\mu\Omega$ cm)	Vickers hardness (GN/m^2)	Estimated insulator thickness (Å)	ρ_t[a] ($\mu\Omega$ cm^2)
Ag[b]	Metz	1.6	0.26	10[c]	0.3
Ni[b]	Novamet	6.9	0.69	25[c]	3.0
Al[b]	Alfa	2.6	0.18	50[d]	3000
Cu[b]	Aldrich	1.7	0.39	50[d]	3000
Substrates for coated fillers:					
TiO_2	Mitsubishi	...	9.00[e]	...	...
Phenolic resin	Mitsubishi	...	0.05[f]	...	...

[a]All values taken from Fig. 1, based on two times the given film thickness.
[b]All values (except as noted) from Ref. 18.
[c]Values from product literature.
[d]Values from Ref. 16.
[e]Values from Ref. 24.
[f]Values from Ref. 25.

ρ_{core} is the resistivity of the core material. Since information regarding the coating thickness on a powder is often more easily attainable than the volume fraction, it may be more convenient to express Eq. (15) in terms of the coating thickness; V_{coat} ($= 1 - V_{core}$) is related to the coating thickness τ by the following:

$$V_{coat} = (d^3 - 3d^2\tau + d\tau^2 + \tau^3)/d^3. \quad (20)$$

Thus, for coated fillers, we substitute Eqs. (19) and (20) for R_i in the model. Since the coatings are normally quite thin relative to the particle size, the physical properties (E, H, and ξ) of the substrate material, rather than the coating material, should be used in the model, while the electrical properties (ρ_i and ρ_t) of the coating material should be used.

IV. EXPERIMENTAL VERIFICATION OF THE MODEL

A. Experimental procedure

Several different filler materials were used in this investigation to determine the accuracy of the model for resistivity. These materials, along with the physical properties used in the calculations, are listed in Table II. Relatively monosize distributions of all powders were used; all powders were roughly spherical. Several different volume fraction loadings were made for each powder; when the resistance of a sample no longer decreased appreciably with additional filler loading, this resistance was taken to be the resistance of the sample. Continued loading of filler beyond this bottom end volume fraction results in highly porous samples with poor mechanical properties but no improvement in resistivity. Silicone rubber (G.E. 845 silicone elastomer) was the polymer matrix material used in this investigation.

After weighing all samples to the proper volume loading using a mixture of about 16% silicone in trichloroethylene (TCE) solvent the batches were mixed for 1 min with a polypropylene propeller blade at 800 rpm. The slip was cast onto 6×8 in.^{2} borosilicate glass sheets into 250–300 μm sheets and cut into 2×5 cm^2 rectangular samples.

The dc electrical resistance of three to six samples of each formulation and thickness was measured across each sample by a four-probe measurement technique using the gold-plated leads and a fluke digital multimeter. The resistivity was calculated using the measured sample thickness while the length and width of the samples were held constant at 5.0 and 2.0 cm, respectively. Resistivities for volume fractions other than 0.524 were predicted by multiplying the predicted resistivity by 0.524/(volume fraction), thus compensating for the lesser number of conductive pathways at volume fractions less than 0.524. For all cases, a nominal value of $\sigma_i = 5.0 \times 10^8$ N/m^2 was assumed; this was approximated from the data for previous samples. This value of σ_i was not verifiable but is greater than the elastic yield strength for the Ag and Ni fillers ($\sigma_y = 5$–7×10^7 N/m^2 for Ag and Ni) so the assumption of plastic deformation of the filler in these composites was valid.

B. Results and discussion: Comparison to model

Table III shows how the calculated resistivities for some of the filler materials compares to the predicted resistivities at the given volume fraction, using the material parameters from Table II.

Good agreement was seen for Ag- and Ni-filled composites, but Cu and Al were off by several orders of magnitude. This was probably due to the presence of a much thicker oxide layer on the Cu and Al powders than the value reported in Table II; the values of transient oxide thickness for a given metal are highly dependent on the oxidizing conditions. Powders that have spent years on the shelf in humid and/or corrosive atmospheres would be expected to have thick oxide layers. Quantifying this oxide for an individual powder is not a trivial matter, and requires very sophisticated and expensive analytical equipment, such as electron spectroscopy for chemical analysis or secondary-ion mass spectroscopy, along with a skilled operator.

The Ag-coated fillers showed reasonably good agreement with the model as well, indicating that the assump-

TABLE III. Comparison of predicted resistivities with experimental data, based on Eq. (16a) and the material parameters given in Table II ($\sigma_i = 5 \times 10^8$ N/m^2).

Filler	Particle size (μm)	Vol %	$\rho_{predicted}$ (mΩ cm)	ρ_{exp} (mΩ cm)	Standard deviation (mΩ cm)
Ag	0.5	10	19.0	31.0	±7.50
	0.5	15	13.0	12.0	±3.60
	1.0	15	6.40	7.10	±0.13
	1.0	20	4.80	2.90	±1.90
	5.0	20	0.96	0.49	±0.015
	5.0	25	0.77	0.21	±0.077
	9.0	30	0.36	0.67	±0.036
	9.0	35	0.31	0.40	±0.048
Ni	1.0	20	180	190	±41.0
	1.0	25	140	80	±9.9
Al	5.0	25	110 000	5 100 000	±140 000
	5.0	30	88 000	690 000	±32 000
Cu	1.0	25	110 000	1.5×10^{11}	$\pm 6.1 \times 10^{10}$
	1.0	30	95 000	6.7×10^{10}	$\pm 4.9 \times 10^{10}$
Ag:Ni	5.0	25	2.10	19.0	±0.66
Ag:Ni	5.0	30	1.70	3.70	±0.50
Ag:PR	15	40	0.23	3.80	±0.072
Ag:PR	15	45	0.20	1.70	±0.084
Ag:PR	15	50	0.19	0.98	±0.026
Ag:TiO_2	1.0	20	170.0	61.0	±19.0
Ag:TiO_2	1.0	25	130.0	16.0	±1.7

tion that the mechanical properties of the substrate material and the electrical properties of the coating material controlled the composite resistivity was accurate.

V. CONCLUSIONS

The steady-state model for the resistivity minima of composites is based on the notion that the composite is the result of a series of a large number of resistors combined in series and parallel. There are three separate contributions to the resistance: constriction resistance at the contacts, tunneling resistance at the contacts, and the intrinsic filler resistance through each particle. Tunneling resistance generally dominates the magnitude of the overall resistance; the intrinsic filler resistance becomes significant for conductor-coated insulating filler.

The model-predicted resistivity increases with increasing filler hardness and/or elastic modulus and insulating film thickness, while resistivity decreases with increasing particle size and intrinsic stress. Ag and Ag-coated fillers provided the best combination of low tunneling resistivity and low filler hardness. For the silicone elastomer used, the exact origin of the contact force was unknown but believed to have been provided by a combination of intrinsic stress due to thermal-expansion differences in the matrix, capillary forces between particles, and crosslinking shrinkage. Comparison of the model to experimental data showed that good agreement could be obtained for filler materials in which the tarnish layer was a known quantity for a given powder; for other cases, the experimental values were higher than predicted.

ACKNOWLEDGMENTS

The authors would like to thank the Ben Franklin Partnership and Elastomeric Technologies for their support of this research.

[1] R. L. Opila and J. D. Sinclair, Ann. Proc. Reliab. Phys. Symp. **23**, 164 (1985).
[2] G. E. Pike, Sandia Laboratory Technical Report 81-0263, 1981.
[3] K. A. Hu, D. Moffatt, J. Runt, A. Safari, and R. E. Newnham, J. Am. Ceram. Soc. **70**, 583 (1987).
[4] L. L. Rohlfing, R. E. Newnham, S. M. Pilgrim, and J. Runt, J. Wave Mater. Int. **3**, 273 (1988).
[5] S. Yoshikawa, T. Ota, and R. E. Newnham, J. Am. Ceram. Soc. **73**, 263 (1990).
[6] S. K. Bhattacharya, *Metal-Filled Polymers* (Marcel-Dekker, New York, 1986).
[7] G. R. Ruschau, R. E. Newnham, J. Runt, and B. E. Smith, Sens. Act. **20**, 269 (1989).
[8] S. Kirkpatrick, Rev. Mod. Phys. **45**, 574 (1973).
[9] R. Landauer, in *Electrical Transport and Optical Properties of Inhomogeneous Media*, edited by J. C. Garland and D. B. Tanner (American Institute of Physics, New York, 1978).
[10] Z. Hashin, J. Comp. Mater. **2**, 284 (1968).
[11] D. S. McLachlan, M. Blaskiewicz, and R. E. Newnham, J. Am. Ceram. Soc. **73**, 2187 (1990).
[12] T. R. Shrout, D. Moffatt, and W. Huebner, J. Mater. Sci. **26**, 145 (1991).
[13] S. K. Bhattacharya, A. S. Basu, and K. D. Sadhan, J. Appl. Poly. Sci. **25**, 111 (1980).
[14] G. R. Ruschau, S. Yoshikawa, and R. E. Newnham, Intl. J. Hybrid Microelectron. **13**, 100 (1990).
[15] R. Holm, *Electric Contacts* (Springer, Berlin, 1967).
[16] U. R. Evans, *The Corrosion and Oxidation of Metals: First Supplementary Volume* (St. Martin's, New York, 1968).
[17] I. Dietrich, Z. Phys. **132**, 231 (1952).
[18] H. Wagar, *Physical Design of Electronic Systems* (Prentice Hall, Englewood Cliffs, NJ, 1971), Vol. 3.
[19] N. Yasuda and M. Nagata, in Proceedings of the First International Hybrid Microelectronics Symposium, Japanese Branch, edited by T. Soto, 1985, p. 90.
[20] L. E. Nielsen and T. B. Lewis, J. Poly. Sci. A **2**, 1705 (1969).
[21] L. E. Nielsen, *Mechanical Properties of Polymers and Composites* (Marcel-Dekker, New York, 1974).
[22] R. M. German, *Particle Packing Characteristics* (Metal Powders Industries Federation, Princeton, NJ, 1989).
[23] B. Miller, J. Appl. Poly. Sci. **10**, 217 (1966).
[24] W. J. Lackey, D. P. Stinton, G. A. Cerny, A. C. Schaffhauser, and L. L. Fehrenbacher, Adv. Ceram. Mater. **2**, 24 (1987).
[25] R. A. Flinn and P. K. Trojan, *Engineering Materials and Their Applications* (Houghton Mifflin, Boston, 1981).